POLISH MARITIME RESEARCH 4 (108) 2020 Vol. 27; pp. 80-90
10.2478/pomr-2020-0068

A NUMERICAL AND EXPERIMENTAL STUDY OF MARINE HYDROGEN–NATURAL GAS–DIESEL TRI–FUEL ENGINES

Rui Zhao[1]
Leping Xu[1]
Xiangwen Su[2]
Shiquan Feng[3]
Changxiong Li[1]
Qinming Tan[1]
Zhongcheng Wang1
[1] Merchant Marine College, Shanghai Maritime University, China
[2] CSSC-MES Diesel Co. Ltd, Shanghai, China
[3] School of Automotive Engineering, Changshu Institute of Technology, Suzhou, China

ABSTRACT

Maritime shipping is a key component of the global economy, representing 80–90% of international trade. To deal with the energy crisis and marine environmental pollution, hydrogen-natural gas-diesel tri-fuel engines have become an attractive option for use in the maritime industry. In this study, numerical simulations and experimental tests were used to evaluate the effects of different hydrogen ratios on the combustion and emissions from these engines. The results show that, in terms of combustion performance, as the hydrogen proportion increases, the combustion ignition delay time in the cylinder decreases and the laminar flame speed increases. The pressure and temperature in the cylinder increase and the temperature field distribution expands more rapidly with a higher hydrogen ratio. This means that the tri-fuel engine (H_2+CH_4+Diesel) has a faster response and better power performance than the dual-fuel engine (CH_4+Diesel). In terms of emission performance, as the hydrogen proportion increases, the NO emissions increase, and CO and CO2 emissions decrease. If factors such as methane escape into the atmosphere from the engine are considered, the contribution of marine tri-fuel engines to reducing ship exhaust emissions will be even more significant. Therefore, this study shows that marine hydrogen-natural gas-diesel tri-fuel engines have significant application and research prospects.

Keywords: hydrogen; tri-fuel engine; combustion performance; emission performance

INTRODUCTION

The major advantages of maritime transportation, such as large volume and low cost, have enabled maritime shipping to become a key component of the global economy, representing 80–90% of international trade [1]. Given its sheer scale, the maritime sector contributes significantly to global ecological impacts [2, 3]. In the past few decades, people have become increasingly sensitive about environmental protection due to the growing energy crisis and environmental problems [4]. Different organizations, such as the International Maritime Organization (IMO) and governments of various countries, have introduced pollutant restriction regulations and set up emission control zones to protect the marine environment and effectively control the emission of harmful gases. Among them, IMO's Annex VI of MARPOL 73/78, "Regulation for the prevention of air pollution from ships" has imposed strict limits on exhaust gas emissions from ship engines, laying out the standards for the required reduction in ship exhaust emissions and their time frames [5].

At present, liquefied natural gas (LNG) has become the first choice alternative fuel for marine engines thanks to its environmental benefits [6]. However, LNG-fuelled engines suffer from a slight power loss and other disadvantages due to the low combustion rate and long combustion duration of natural gas. Consequently, LNG-fuelled ships will be unable to meet the increasingly strict requirements imposed on ship emissions and conform to the IMO shipping regulations to reduce CO_2 emissions in 2050 to 50% of the 2008 levels. Based on the characteristics of the marine engine's actual working environment, adding hydrogen (H_2) to the fuel used in a marine LNG-diesel dual-fuel engine and converting it to a hydrogen-natural gas-diesel tri-fuel engine can increase the power and reliability. H_2 is a very flammable gas with a fast-burning rate. It is also recognized as a clean energy source and known as the most promising secondary energy source in the 21st century [7]. The latest developments in the electrolytic industry will increase the attractiveness and practicality of renewable energy sources, such as wind power and hydropower, for obtaining hydrogen via water electrolysis [8].

Since this topic is very important and has scientific potential, in recent years, some scholars have carried out research work on hydrogen-natural gas-diesel tri-fuel engines and have achieved many beneficial results. Wojciech Tutak et al. [9] studied the dual-fuel engine driven by diesel and hydrogen-rich natural gas through experiments; analysed the influence of the hydrogen ratio on combustion, heat release, combustion stability and exhaust emissions; and pointed out that hydrogen enrichment can improve the combustion process. Ouchikh et al. [10] studied the effect of adding hydrogen to natural gas in dual-fuel mode on improving combustion performance and engine performance through experiments and pointed out that hydrogen-rich in natural gas usually improves the combustion of gaseous fuel. Abu-Jrai et al. [11] transformed a diesel engine into an engine that can burn three fuels (H_2, CH_4 and traditional diesel) at the same time, carried out experimental research, and pointed out that gaseous fuels (H_2 and CH_4) affected the heat release rate and the NOx and PM emissions. Abu Mansor et al. [12] used ANSYS FLUENT to calculate and analyse the effect of changing the hydrogen-methane-diesel mixing ratio on the pressure, temperature, and NO and CO products in the cylinder. The study concluded that a mixture of 70% hydrogen and 30% methane in all fractions of diesel achieved the best balance between combustion, cylinder operation, and emission characteristics. Alrazen et al. [13] conducted CFD modelling on a single-cylinder engine and calculated the combustion characteristics and emission performance of an H_2-CNG-diesel engine under different fuel gas mixture ratios (H30-N70, H50-N50, and H70-N30) through numerical simulation. Talibi et al. [14] analysed the effects of burning methane-hydrogen mixture on the exhaust emissions of the compression ignition engine and the gas composition in the cylinder. Studies have shown that when burning methane-hydrogen mixtures, the emissions of carbon dioxide and particulate matter in the exhaust gas are both lower, and the emissions of CO and unburned THC are higher compared to diesel fuel alone. The NOx emissions increase as the proportion of hydrogen in the mixture increases. Tangoz et al. [15] studied the impact of different compression ratios (9.6, 12.5, and 15) engine power performance and emission characteristics. Their study suggested that when the CR value is 9.6, a 5 or 10% hydrogen ratio can be used to enhance the power performance and emission performance of a diesel engine. Mahmood et al. [16] designed and tested a gas mixer (CNG-H2-AIR Mixer) that mixes natural gas, hydrogen, and air. Through simulation calculations, the gas mixer is suitable for mixing air with compressed natural gas (CNG) and a mixture of hydrogen and compressed natural gas (HCNG), and it can provide a mixture with a high uniformity index to accurately control the air to gas fuel ratio at different engine speeds.

The current research mainly involves small engines and has made outstanding contributions to the research on this type of engines. However, there is little research on applying the tri-fuel model to large engines in the maritime field. The purpose of this study is to use numerical simulations and bench experiments to compare the combustion and emission performance with respect to different proportions of hydrogen in the gaseous fuel and study the possibility of hydrogen-natural gas-diesel tri-fuel engines as marine engines. The research results can be used for exploring designs for future marine engines.

METHODOLOGY OF THE NUMERICAL AND EXPERIMENTAL STUDIES

NUMERICAL METHOD

In this study, a numerical simulation method was used to analyse the effects of hydrogen addition on combustion and exhaust emissions in a tri-fuel engine cylinder. First, the chemical reaction kinetics analysis software CHEMKIN was used to perform the numerical calculations. Using proven chemical kinetics mechanisms [17], the effects of different fuel mixture ratios on combustion characteristics, such as ignition delay time, peak gas temperature and laminar flame speed, were studied. Then, the AVL-Fire simulation package was used to build a 3D engine model, and the effects of different fuel mixture ratios on cylinder pressure; cylinder temperature; cylinder temperature field distribution; and NO, NO_2, CO, and CO_2 emissions were calculated. In the following, we explain the chemical kinetics and 3D engine models.

1) Chemical kinetics model

In this study, the closed homogeneous 0-D reaction model, i.e., closed homogeneous reactor based on the constant volume bomb model, available in CHEMKIN was used to simulate the ignition delay time and maximum temperature of the three fuel mixtures. The calculation model for flame propagation speed, including a gas input port, a flame speed calculator, and an output port in CHEMKIN was used to calculate the laminar flame speed of the three fuel mixtures. Since pure diesel is a multi-component mixture, it is difficult to fully reflect it in chemical kinetics calculations. Some alternative components are needed in numerical studies. N-Heptane (nC_7H_{16}) has a cetane number comparable to diesel and chemical properties similar to diesel fuel; it is commonly used in research to study the combustion performance of diesel [18]. The main component of natural gas is methane (CH_4) with a volume fraction of about 96%, and it is generally used to study the combustion performance of natural gas. Therefore, in this study, a mixture of n-heptane (nC_7H_{16}), CH_4 and H_2 was used for calculating combustion in CHEMKIN. In the simulation process, the proportions of oxygen and nitrogen in each component of the mixture and the ratio of H_2-CH_4 mixed gas to n-heptane remained unchanged. The gas-fuel replacement rate was about 90%. In the simulations, the reaction time was set to 0.05 sec, initial reaction temperatures of 500, 600, 700, 800, 900, and 1000 K were used, the initial reaction pressure was set to 20 atm, i.e., 2.0265 Mpa, and the equivalent ratio was 1. The flame propagation velocities were calculated under seven different operating conditions, where the proportion of hydrogen in the H_2-CH_4 mixture in these operating conditions was 0, 5, 10, 15, 20, 25, and 30%, respectively. From the calculation results, the ignition delay time, laminar flame speed, and maximum temperature of the three fuel mixtures were recorded.

2) 3D engine model

To evaluate the effects of varying hydrogen ratios on the in-cylinder pressure; in-cylinder temperature; emission rates of NOx, CO, and CO_2; and in-cylinder temperature field distribution in a marine hydrogen-natural gas-diesel tri-fuel engine, a 3D simulation model should be established. This paper establishes a 3D engine simulation model, taking the marine engine MAN B&W 6L23/30DF as reference. This type of marine engine completed the Type Approval Test (TAT) and the IMO Tier III emission certification test in 2017. Table 1 shows the relevant structural parameters of the original diesel engine under full load.

Tab. 1. Parameters of the Engine for 3D Model

Make &Model	MAN B&W 6L23/30
Number of Strokes	4
Bore	225 mm
Stroke	300 mm
Displacement Volume	11.9 L
Rated speed	750 r/min
Compression Ratio	13.5
MCR Power	1000 kW
MCR Fuel Consumption	183 g/kWh
Piston Speed	7.5 m/s
Number of Injection Holes	8
Maximum Combustion Pressure	17 MPa
Mean Effective Pressure	1.56 MPa

The combustion chamber meshing needs to be performed before the numerical calculation. As there are eight injection holes on the injection head, only a 45° engine cylinder model can be established to save calculation time. Considering the computing power, the intake and exhaust valves are not considered in this article. This will affect the initial swirl and tumble in the cylinder after the intake is completed. Although this initial swirl and tumble will affect the spray combustion process, the impact on the overall combustion trend is not particularly obvious. Previous simulation calculations were performed on the full-cylinder model. In this paper, the initial state vortex is 1400. That is, the swirl intensity is 1400 r/min, the rotation point is (0 0 0), and the rotation direction is (0 0 1). This setting was also applied to the eighth model in this article. The cylinder simulation model shown in Fig. 1 consists of the piston at the top dead centre. In this study, AutoCAD was used for 2D geometric modelling. The established model was imported into the Fire ESE Diesel module of the AVL-Fire software to build a 3D mesh model. The cylinder wall heat loss was calculated using the model developed by Han and Reitz [19]. The RNG κ–ε model [20] was used to simulate turbulence in the cylinder, the Dukowicz model was used for droplet evaporation [21], and a standard wall function was used for the wall heat transfer model. The Rayleigh-Taylor (KH/RT) [22] hybrid model was also used. The KH decomposition model was used to draw small droplets from the ejector within the specified breakup length, but the ejector still maintains its dense liquid core. If the length exceeds the breakup length, the RT model was used in combination with the KH model to predict the secondary breakup [23]. The initial diameter of the droplets (0.00025 m) were in the range of the nozzle hole diameter (0.00033 m), which is a characteristic of high-pressure injection systems. The cause of instabilities leading to spray breakup is the amplification of disturbances generated under injection, hydrodynamic impact forces, and the interaction of a liquid sheet with the surrounding gas. When the waves generated by the disturbances reach a critical amplitude, the sheet fragments contract into ligaments and break down into drops. The KH model was the primary jet breakup, and the KH/RT model was used to calculate the sudden droplet breakup. The number of grids at the time of intake valve closure was 54,016, and a grid independence test was performed. In the simulation model, when the chemical reaction was activated after diesel injection, the temperature of the diesel-air mixture in the cylinder reached 600 K, the temperatures of the cylinder head and cylinder wall were set to 465 K, and the initial temperature of the piston was set to 525 K.

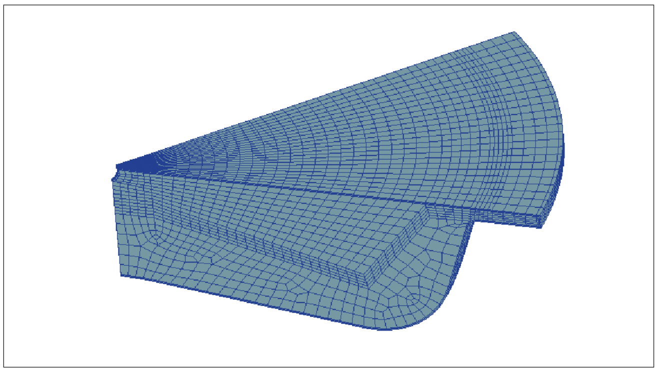

Fig. 1. Sector meshes used in engine simulation

To simulate the effects of different ratios of H_2 and CH_4 on combustion and emissions in the engine cylinder, according to the ratio of energy, the ratios of hydrogen and methane are 0:100, 10:90, 20:80 and 30:70, respectively. Taking the MCR point of L23/30H as the calibration condition, the total energy input corresponding to the specific fuel consumption at this condition point was calculated and assumed constant. Mixed gas fuel (H_2 and CH_4) accounts for 75% of its energy. Then, according to the ratio based on energy, the ratio of the mixed gas was changed to ensure that the total energy was constant. Other parameters in the model remained unchanged. The diesel injection time was nine degrees before top dead centre (TDC), and the diesel injection amount per cylinder was 0.28 g/cycle. The thermal parameters of the engine at 750 rpm and 750 kW were used for initializing the above 3D model, and the entire process from closing the intake valve to opening the exhaust valve was simulated.

First, the accuracy of the numerical calculation chemical model was guaranteed by the ignition delay and laminar flame velocity derived from the mechanism before the 3D calculation. Then, based on the verified mechanism, the 3D simulation model of the cylinder was established to verify the numerical calculation physical model (such as spray crushing or the wall surface thermal model). The simulation results using zero gas substitution rate (H_2 0%, CH_4 0%, nC_7H_{16} 100%) were compared with the experimental cylinder pressure under pure diesel. The calculated in-cylinder pressure curve obtained from the simulation was compared with the experimental curve shown in Fig. 2. The two curves are basically coincident, and the largest divergence occurs at the crank angle position corresponding to the maximum in-cylinder pressure. The maximum in-cylinder pressures for experiment and simulation were 13.96 MPa and 14.42 MPa, respectively, i.e., a deviation of only 3%. Figure 2 reflects the correctness of the model indirectly. The 3D model is feasible and can be used for numerical simulation to evaluate the effect of engine performance and emissions under different hydrogen ratios. Moreover, the trends reflected in the numerical simulation results and the experimental data can be mutually confirmed.

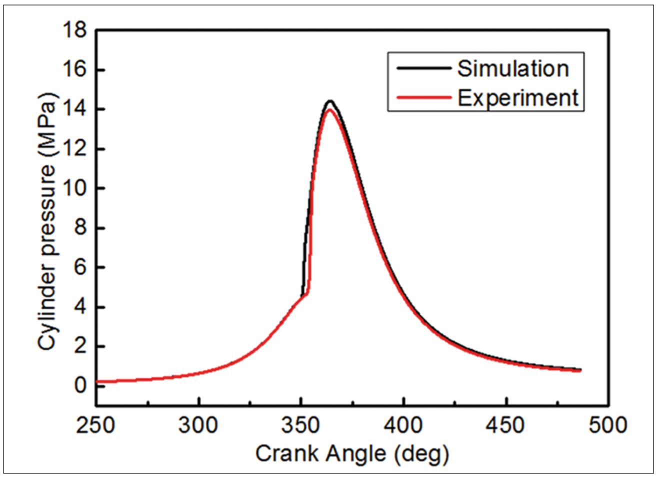

Fig.2. Comparison of experimental and calculated cylinder pressure values

EXPERIMENTAL METHOD

It is difficult to carry out hydrogen-natural gas-diesel tri-fuel mixed combustion experiments on the marine engine MAN B&W 6L23/30DF. This is because the marine engine is too large to complete this experiment, and it is still difficult to transform the hydrogen fuel supply system. As a last resort, in this study, a single-cylinder engine was transformed into a tri-fuel mixed-fired engine test bench. In the experimental study, the trend of exhaust gas emissions changing with increasing hydrogen ratio could be obtained. This trend formed a correspondence with the trend found in numerical research and has a reference value. The experimental setup is shown in Fig. 3. In this experiment, the methane-hydrogen mixture was passed into the main intake pipe through a branch intake pipe. The mixture was further mixed with air and, subsequently, it entered the engine cylinder. The original engine used in the experiment was a ZR180 single-cylinder diesel engine and its parameters are shown in Table 2. The dynamometer was a ZF100KB magnetic particle dynamometer, and it was equipped with a dynamometer control cabinet and a fuel consumption meter.

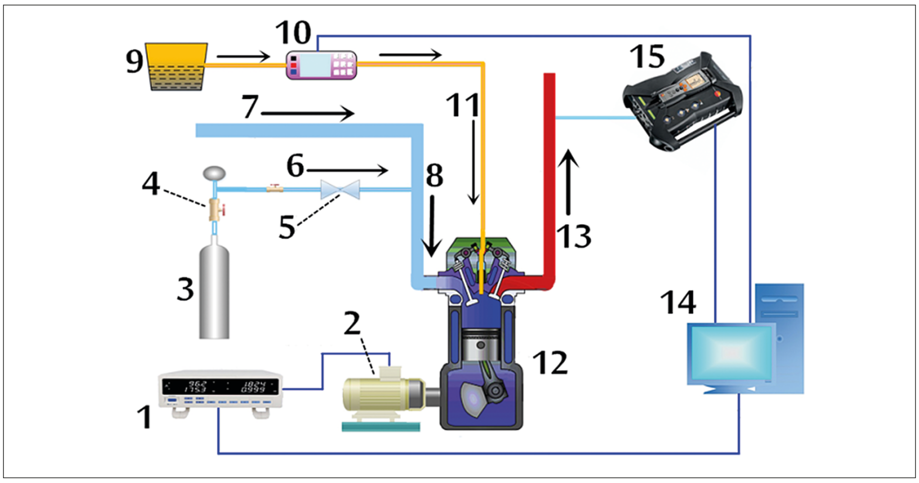

Fig.3. Diagram of the experimental system // 1. Dynamometer control cabinet, 2. Permanent magnet synchronous dynamometer, 3. Cylinder filled with gas fuel ($CH_4 + H_2$), 4. Flow regulating valve, 5. Check valve, 6. Intake manifold ($CH_4 + H_2$), 7.Fresh air duct tube, 8. Intake main, 9. Fuel tank, (diesel), 10. Fuel consumption monitor, 11. Fuel rail, 12. Single-cylinder engine, 13. Exhaust emission, 14. Computers for control and data collection, 15. Testo 350 combustion gas analyser

Tab.2. Parameters of the test bench engine

Make &Model	CHANGCHAI ZR180
Number of Cylinders	Single cylinder
Type of cooling	Air cooling
Intake Type	Naturally aspirated
Type of Injection	Direct Injection
Injection Pressure	22–23 MPa
Bore	80 mm
Stroke	80 mm
Swept Volume per Cylinder	0.402 L
Compression Ratio	19.5
Rated Power	5.67 kW
Rated Speed	2600 r/min

The emissions measurement device in the experiment was a Testo 350, a portable combustion gas analyser made in Germany. It can detect NO, NO_2, CO, and CO_2 concentrations, as well as exhaust temperature. The measurement parameters are shown in Table 3.

Tab.3. Parameters of the Testo 350 combustion gas analyser

Parameters	Range	Accuracy
O_2	0–25 Vol.%	0.01 Vol.%
NO	0–4000 ppm	1 ppm
NO_2	0–500 ppm	0.1 ppm
CO	0–10000 ppm	1 ppm
CO_2	0–50 Vol.%	0.01 Vol.%

In this study, the engine speed was fixed at 1000 rpm, and the exhaust emission parameters of each fuel mixture ratio at seven output powers were recorded. The seven output powers were 1200, 1600, 2000, 2400, 2800, 3200, and 3600 W. The recorded engine emission parameters were NO, NO_2, CO, and CO_2 gas emissions and exhaust temperature. The hydrogen and methane mixture used in the experiment was prepared by a special gas manufacturer, and the natural gas was replaced with 99.9% purity CH_4. The ratio of hydrogen and methane was 0:100, 5:95, 10:90 and 15:85, respectively. When the ratio of hydrogen to methane was increased to 20:80, the engine knock was very violent, and the higher hydrogen ratio experiments (20, 25, and 30%) could not be performed. Nevertheless, the trend of increasing the proportion of hydrogen on the engine has become apparent. The pressure is 12 MPa, and the flow rate of the mixture is 2.5 L/min. The flue gas analyser automatically records data and fuel consumption rate every 0.5 seconds and once after the experiment reached stable operating conditions. Each measurement was averaged and used to evaluate diesel emissions.

RESULTS AND DISCUSSION

COMBUSTION CHARACTERISTICS

1) Ignition delay time

The ignition delay time represents the time required for the fuel to reach the ignition condition starting from the initial state. It is an important parameter for characterizing the ignition characteristics of the fuel. A shorter ignition delay time signifies a faster engine response. The temperature, pressure, and changes in the free radical emission spectrum intensity can be used to define the ignition delay time. For hydrocarbons, the ignition delay time is usually expressed using the Arrhenius equation [24]. According to this equation, the ignition delay time is expressed in terms of temperature and concentration of each reactant, as follows:

$$\tau = A[Fuel]^{\alpha}\,[O_2]^{\beta}\,[M]^{\gamma}\,e^{-\frac{E}{RT}} \tag{1}$$

In (1), A is the pre-factor; $[Fuel]$ and $[O_2]$ represent the molar concentration of substance *fuel and oxygen*; M is the third gas, such as N_2, Ar, etc.; α, β and γ are the factors affecting the aforementioned parameters and E is the activation energy.

The ignition delay time curves versus different hydrogen ratios are shown in Fig. 4, where the left, middle and right y-axes correspond to the initial temperatures of 800, 900 and 1000 K, respectively.

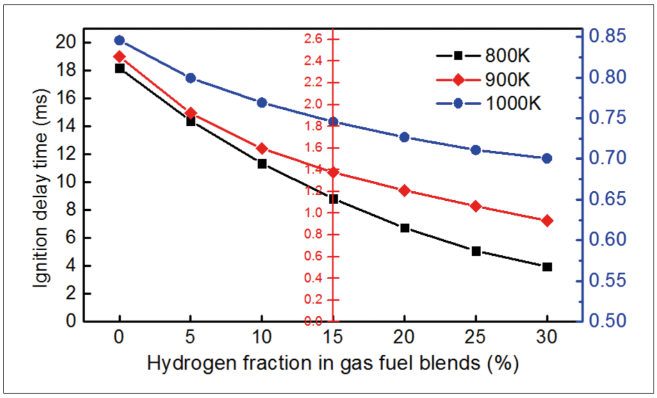

Fig.4. Ignition delay times versus varying hydrogen ratios at different temperatures in numerical simulations

It can be observed in Fig. 4 that under the same initial temperature, the higher the proportion of hydrogen, the shorter the ignition delay time. For example, when the initial temperature was set to 900 K, the ignition delay times for seven different hydrogen proportions were 2.442, 1.920, 1.596, 1.376, 1.211, 1.065, and 0.787 ms. This result means that the tri-fuel engine (H_2+CH_4+Diesel) has a faster response time compared to the dual-fuel engine (CH_4+Diesel). This is due to the different physical and chemical properties of the three fuels. Hydrogen requires the lowest ignition energy and has the best flame propagation and the highest low heating value. Therefore, the addition of hydrogen increases the fuel reaction activity, which shortens the ignition delay time. This results in improving the engine ignition performance, shortening the flame retardation period, and a smooth engine start.

2) Laminar flame speed

Laminar flame speed is an important parameter for characterizing the combustion process of internal combustion engines. A high laminar flame speed of the fuel means that the combustion process is close to the ideal constant volume heating cycle and, consequently, the internal combustion engine can obtain higher thermal efficiency [25].

Significant research has been carried out on the theoretical aspects of laminar flame, and Mallard and Le Chatelier described laminar flame as early as 1883. The propagation velocity of the laminar flame is mainly related to the type of fuel, air-fuel ratio, temperature, and pressure. The laminar flame speed can be approximated using the following expression:

$$S_L \approx \overline{T}^{0.375}\, T_u\, T_b^{-n/2} \exp\left(-\frac{E_A}{2R_u T_b}\right)^{p(n-2)/2} \qquad (2)$$

In (2), *SL* is the laminar flame speed, *Tu* is the temperature of the unburned gas, *Tb* is the temperature of the combustion gas, *P* is the pressure of the unburned gas, *n* is the total reaction order of the package, E_A is the activation energy and $T = (Tu + Tb)/2$.

The laminar flame speed variation curve under different hydrogen ratios is shown in Fig. 5. A higher initial temperature increases the laminar flame speed. At the same time, the laminar flame velocity increases as the proportion of hydrogen increases. For example, when the initial temperature is 600 K, the laminar flame speed is 125.017 cm/s under tri-fuel mode with 30% hydrogen. However, under dual-fuel mode with 0% hydrogen ratio, the laminar flame speed is 45.121 cm/s. This is due to the good flame propagation velocity characteristics of hydrogen, which increases the combustion speed in the cylinder.

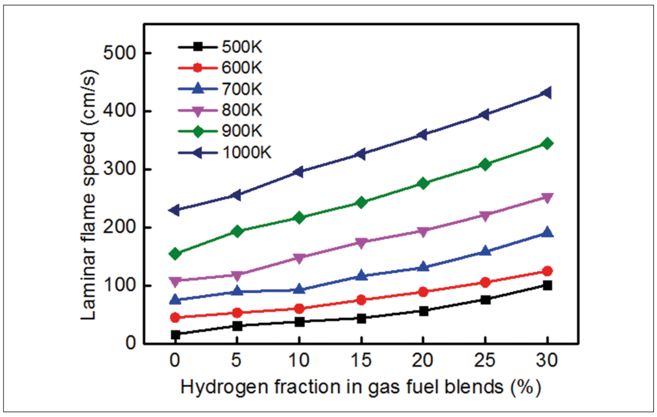

Fig.5. Laminar flame speeds versus varying hydrogen ratios at different temperatures in numerical simulations

The spatial distribution of the cylinder temperature calculated using the 3D engine model also shows that adding hydrogen increases the combustion speed in the cylinder. Figure 6 shows that under the tri-fuel mode (H_2+CH_4+Diesel), the cylinder temperature is higher than that under the dual-fuel mode (CH_4+Diesel). When the crank angle is 364°CA, the high-temperature area in the dual-fuel mode without hydrogen, i.e., 100% CH_4 is much larger than that in the tri-fuel mode, i.e. 30%H_2+70%CH_4. This behaviour is due to the slow combustion of methane. Increasing the hydrogen proportion can increase the combustion speed in the cylinder. It can be seen from the numerical simulations that the combustion speed in the tri-fuel engine cylinder is faster than that in the dual-fuel engine, which improves the combustion efficiency of the engine [26].

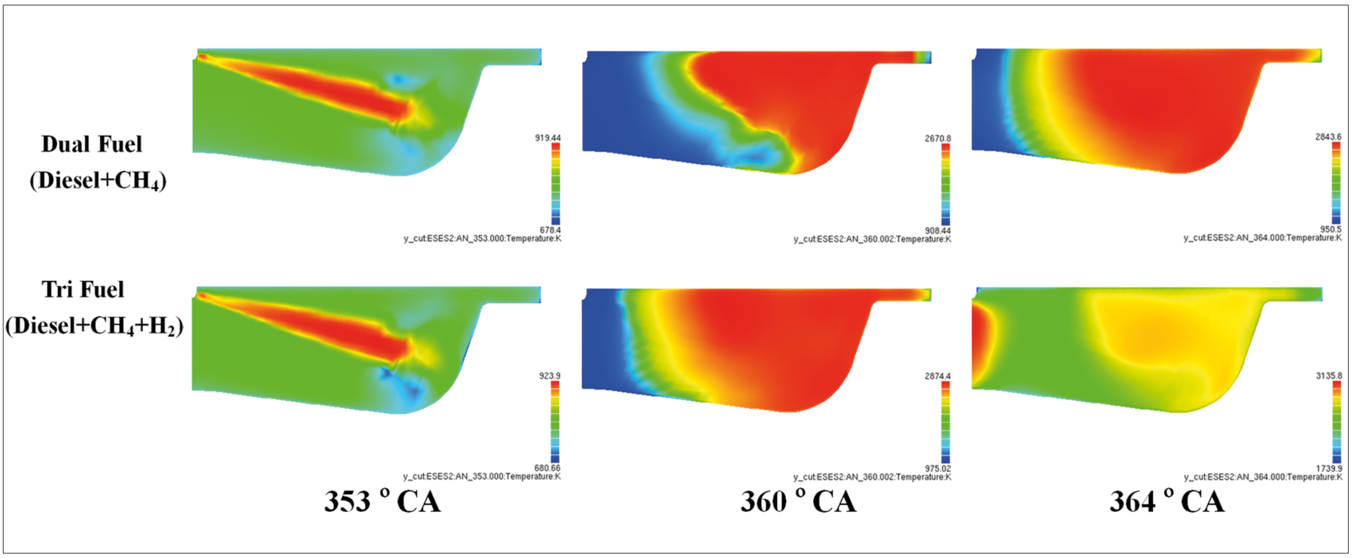

Fig. 6. Temperature distribution of the engine's cylinder at top dead centre positions under different hydrogen ratios

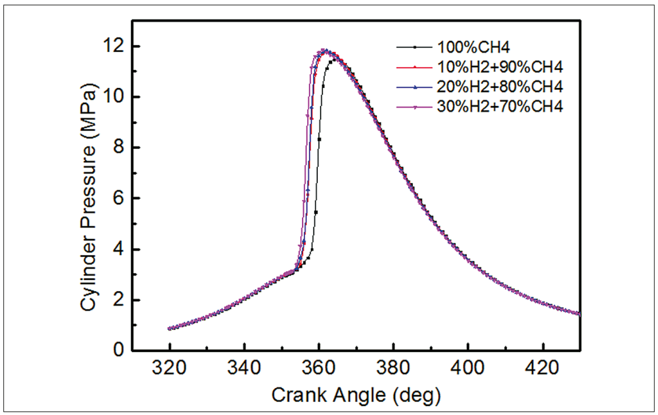

Fig. 7. Effect of varying hydrogen ratios on in-cylinder pressure versus crank angle behaviour in numerical simulations

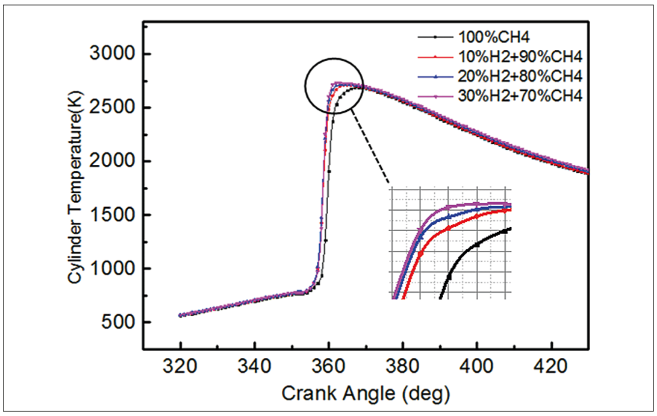

Fig. 8. Effect of varying hydrogen ratios on in-cylinder temperature versus crank angle behaviour in numerical simulations

3) In-cylinder pressure and temperature

Figures 7 and 8 show the curves of the pressure and temperature in the cylinder as a function of crank angle calculated using the 3D simulation model. It can be observed from the figures that the peak cylinder pressure value increases with increasing hydrogen proportion if other parameters in the model remain unchanged. When the ratio between H_2 and CH_4 is 30:70, i.e. 30%H_2+70%CH_4, the peak pressure in the cylinder is the highest. This pressure is 11.85 MPa and the corresponding crank angle is 361°. When the hydrogen ratio increases from 0% to 30%, the entire pressure curve is shifted forward. This shows that as the proportion of hydrogen in the mixed fuel increases, combustion in the cylinder becomes faster. The engine cylinder pressure increases mainly because hydrogen, with excellent combustion characteristics, promotes diesel combustion, accelerates the flame propagation speed in the cylinder and improves combustion efficiency.

Figure 8 shows the curve of the in-cylinder temperature calculated by the 3D model as a function of the crank angle. Similar to the trend shown in Fig. 7, the peak value of the in-cylinder temperature increases as the hydrogen ratio increases when all other parameters remain unchanged. Data from experimental tests confirm this trend, as shown in Fig. 9. The increase in hydrogen in the mixed gas provides improved homogeneity and a better environment for the entire combustion process. As the proportion of hydrogen increases, the engine cylinder has faster combustion and higher temperature, closer to a constant volume, thereby improving the efficiency of the engine [27].

EMISSION

1) NOx emission

Figures 10–12 show the impact of varying hydrogen ratios on NOx emissions from the tri-fuel engine. The curves of the NO and NO_2 produced as a function of the crank angle in the 3D engine simulation model are shown in Fig. 10. The amount of emitted NO increases and the amount of emitted NO_2 decreases when the proportion of hydrogen increases.

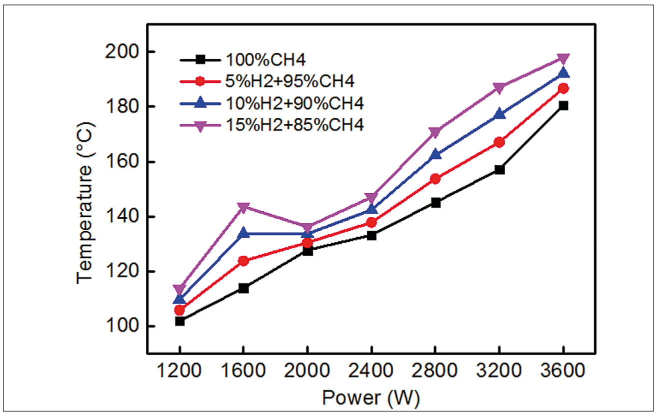

Fig. 9. Effect of varying hydrogen ratios on exhaust gas temperatures versus power behaviour in experiments

Figures 11 and 12 show the NOx and NO concentrations measured in the engine exhaust gas under different operating conditions for the engine experiment. With increasing engine output power, the concentration of NOx in the engine exhaust gas increases. The concentration of NOx emission does not vary significantly with changing proportions of hydrogen. As the output power increases, the difference between the NO emission concentration values for different mixture ratios gradually decreases. This behaviour may be caused by the increase in hydrogen proportion, which increases the temperature in the engine cylinder. The increased temperature promotes the generation of NO, which leads to an increase in NO emissions.

High temperature is a major factor that increases the total NOx emissions. However, the generation of NOx in the engine cylinder is a complicated chemical reaction process, which is not only affected by high temperature but is also related to the oxygen concentration in the environment and the total duration during which the temperature remains high. The proportion of hydrogen affects the NOx emissions in two ways: 1) The increase of the cylinder temperature promotes the generation of NOx, 2) Shortening the combustion time and the water vapour generated by hydrogen combustion suppress the generation of NOx. The specific underlying mechanisms for this behaviour need to be studied further.

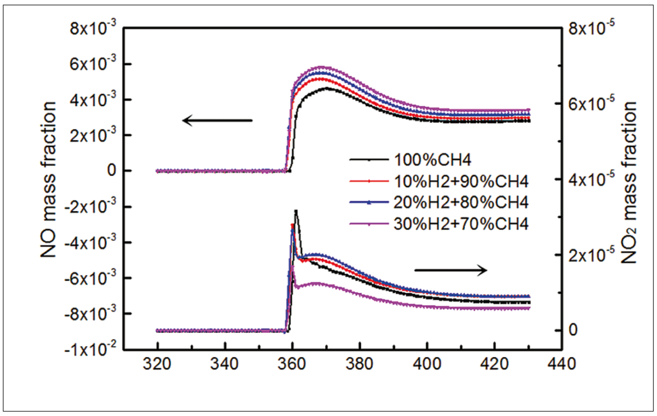

Fig.10. Effect of varying hydrogen ratios on NO and NO2 emissions versus crank angle behaviour in numerical simulations

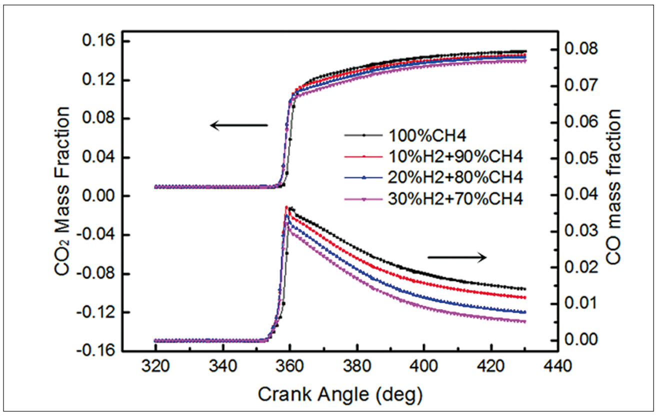

Fig.13. Effect of varying hydrogen ratios on CO and CO2 emissions versus crack angle behaviour in numerical simulations

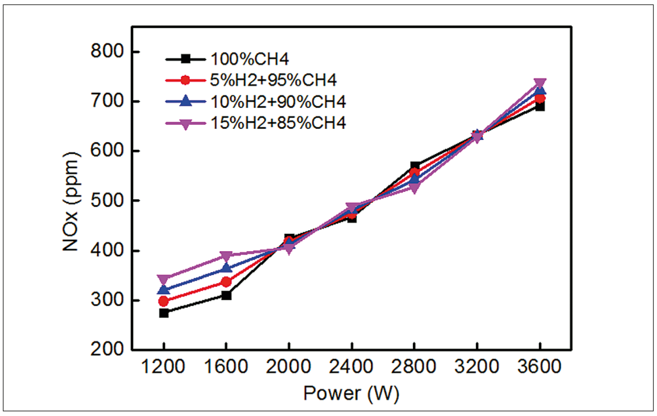

Fig.11. Effect of varying hydrogen ratios on NOx concentration versus power behaviour in experiments

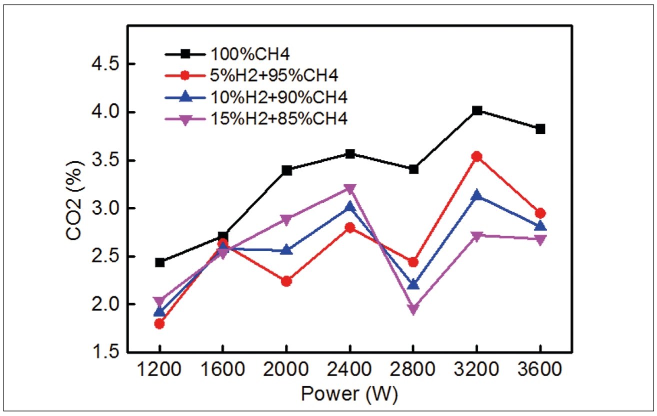

Fig.14. Effect of varying hydrogen ratios on CO2 concentration versus power behaviour in experiments

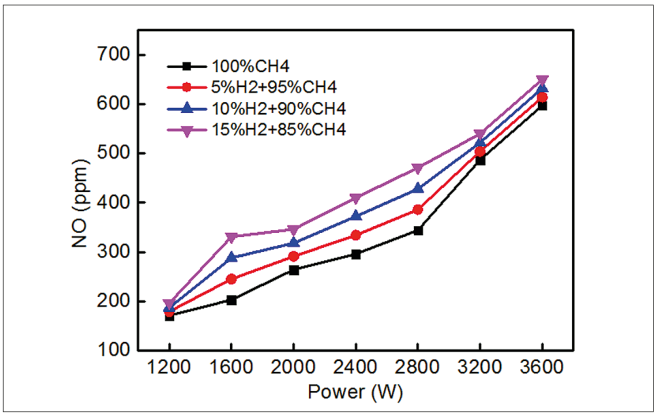

Fig. 12. Effect of varying hydrogen ratios on NO concentration versus power behaviour in experiments

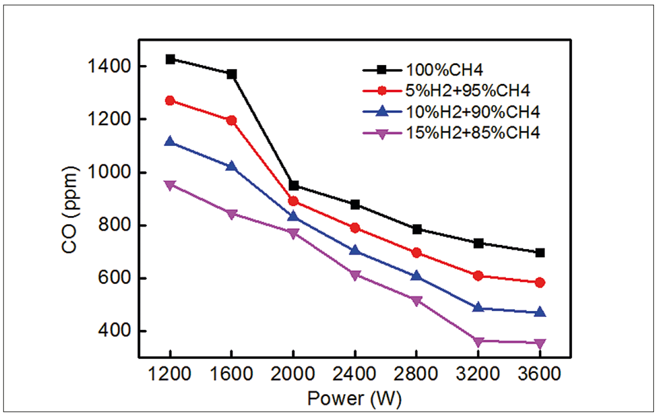

Fig.15. Effect of varying hydrogen ratios on CO concentration versus power behaviour in experiments

2) CO_2/CO emissions

Figures 13–15 show the effects of different hydrogen ratios on CO_2 and CO emissions in tri-fuel engines. Figure 13 shows a curve of the amount of CO_2 and CO generated as a function of the crank angle in the 3D engine model. It can be observed that when the proportion of hydrogen increases, the amounts of CO_2 and CO produced decrease, with the latter showing a significant reduction.

Figure 14 shows the ratio of the CO_2 concentration in the engine exhaust gas under different operating conditions for the engine. Since the engine is naturally aspirated, the lambda parameter becomes smaller as the power increases. The curve in the figure shows that the trend of CO_2 emissions is relatively complicated. However, the emissions when the hydrogen ratio is 0%, i.e. 0%H_2+100%CH_4, are significantly higher than the other three hydrogen ratios. As the output power increases, the advantages of doping fuel with hydrogen gradually become apparent. This is because hydrogen (H_2) does not contain carbon atoms, so the only product of combustion is water (H_2O). The combustion products of fuels such as diesel and methane inevitably contain CO_2. Moreover, methane

(CH_4) in natural gas is also a greenhouse gas. Therefore, replacing part of the natural gas with hydrogen is beneficial for reducing greenhouse gas emissions.

Figure 15 shows the CO concentration in the engine exhaust gas under varying hydrogen ratios. As the engine output power increases, the concentration of CO in the exhaust gas decreases. At the same time, for the same value of output power, a high proportion of hydrogen lowers the CO emission concentration. The data measured by the bench experiments are consistent with the data calculated by the 3D engine model and both show a downward trend.

It is well known that increasing the hydrogen content in fuel can significantly reduce CO_2 emissions, which has great significance for low-carbon shipping. If the methane escape from natural gas engines is considered, the environmental benefits of using hydrogen to partially replace natural gas become even more significant.

CONCLUSIONS

In this study, numerical simulations and bench tests were used to study the marine hydrogen-natural gas-diesel tri-fuel engine. A 3D model of the marine engine MAN B&W 6L23/30DF was established for simulations and a modified single-cylinder tri-fuel co-firing engine test bench was used for experiments. The effects of varying proportions of hydrogen in the fuel on combustion characteristics, i.e. ignition delay time, laminar flame speed, in-cylinder pressure, in-cylinder temperature and temperature field distribution, and NOx/CO/CO_2 emissions were studied. Based on the numerical simulation results and bench tests, the main conclusions are as follows:

1) This type of engine has better combustion characteristics than the natural gas-diesel dual-fuel engine. The ignition delay time of the engine is shortened, the laminar flame speed increases and the pressure and temperature in the cylinder improve due to the good combustion characteristics of hydrogen. Based on the results presented in this paper, the in-cylinder combustion of marine hydrogen-natural gas-diesel tri-fuel engines will be faster and more efficient, which can improve the ship's power performance.

2) The concentration of harmful gases present in the engine exhaust is lower. As the proportion of hydrogen in the fuel increases, the emissions of CO and PM are significantly reduced, and greenhouse gas emissions decrease. If factors such as methane escape into the atmosphere from the engine are considered, the improvement will be even more significant. Based on this paper, it can be concluded that the marine hydrogen-natural gas-diesel tri-fuel engine will have better environmental protection performance.

3) Based on the engine combustion performance and exhaust data obtained from numerical and experimental studies, this type of engine has great application and research prospects. This topic should be further studied by maritime research scholars.

With the rapid development of hydrogen energy technology, these tri-fuel engines will be expected to be applied to ships in the near future. In the next step, we will study how to distribute and regulate each fuel in the application of such engines. In addition, the hydrogen filling and storage issues involving marine hydrogen engines are also worthy of further study.

COMPETING INTERESTS

The authors declare that there are no competing interests in this paper.

ACKNOWLEDGEMENTS

The authors would like to acknowledge the financial support from the Shanghai Government Science and Technology Commission under grant number 17170712100, as well as the financial support of Shanghai Maritime University.

REFERENCES

1. Balcombe P., Brierley J., Lewis C., et al. (2019). *How to Decarbonise International Shipping: Options for Fuels, Technologies and Policies*. Energy Conversion and Management. 182(2), 72–88.

2. Eyring V., Köhler H. W., van Aardenne J., Lauer A. (2005). *Emissions from International Shipping: 1. The Last 50 Years*. Journal of Geophysical Research Atmospheres.110 (D17), 1–12.

3. Lister J., Poulsen R. T., Ponte S. (2015). *Orchestrating Transnational Environmental Governance in Maritime Shipping*. Global Environmental Change. 34, 185–95.

4. Labeckas G., Slavinskas S., Rudnicki J., et al. (2018). *The Effect of Oxygenated Diesel-N-Butanol Fuel Blends on Combustion, Performance, and Exhaust Emissions of a Turbocharged CRDI Diesel Engine*. Polish Maritime Research. 1(97), 108–120.

5. Schinas O., Stefanakos C. N. (2014). *Selecting Technologies Towards Compliance with MARPOL Annex VI: The Perspective of Operators*. Transportation Research Part D-Transport and Environment. 28(28), 28-40.

6. Burel F., Taccani R., Zuliani N. (2013). *Improving Sustainability of Maritime Transport Through Utilization of Liquefied Natural Gas (LNG) for Propulsion*. Energy 57(57), 412–420.

7. Lu J., Zahedi A., Yang C., et al. (2013). *Building the Hydrogen Economy in China: Drivers, Resources and Technologies*. Renewable and Sustainable Energy Review. 23, 543–556.

8. Bicer Y., Dincer I. (2018). *Clean Fuel Options with Hydrogen for Sea Transportation: A Life Cycle Approach*. International Journal of Hydrogen Energy. 43(211), 1179–1193.

9. Tutak W., Arkadiusz, Grab-Rogaliński K., et al. (2020). *Effect of Natural Gas Enrichment with Hydrogen on Combustion Process and Emission Characteristic of a Dual Fuel Diesel Engine*. International Journal of Hydrogen Energy. 1(119), 901–910.

10. Ouchikh S., Lounici M. S., Tarabe, L, et al. (2019). *Effect of Natural Gas Enrichment with Hydrogen on Combustion Characteristics of a Dual Fuel Diesel Engine*. International Journal of Hydrogen Energy. 44(26), 13974–13987.

11. Abu-Jrai A. M., Al-Muhtaseb A. H., Hasan A. O., et al. (2017). *Combustion, Performance, and Selective Catalytic Reduction of NOx for a Diesel Engine Operated with Combined Tri Fuel (H-2, CH4, and Conventional Diesel)*. Energy. 1(119), 901–910.

12. Abu Mansor M. R., Abbood M. M., Mohamad T. I. (2017). *The Influence of Varying Hydrogen-Methane-Diesel Mixture Ratio on the Combustion Characteristics and Emissions of a Direct Injection Diesel Engine*. Fuel. 190(4), 281–291.

13. Alrazen H. A., Abu Talib A. (2016). *A Two-Component CFD Study of the Effects of H-2, CNG, and Diesel Blend on Combustion*. International Journal of Hydrogen Energy 41(24), 10483–10495.

14. Talibi M., Balachandran R., Ladommatos N. (2017). *Influence of Combusting Methane-Hydrogen Mixtures on Compression Ignition Engine Exhaust Emissions snd In-Cylinder Gas Composition*. International Journal of Hydrogen Energy. 42(4), 2381–2396.

15. Tangoz S., Akansu S. O., Kahraman N., et al. (2015). *Effects of Compression Ratio on Performance and Emissions of a Modified Diesel Engine Fueled by HCNG*. International Journal of Hydrogen Energy. 40(44), 15374–15380.

16. Mahmood H. A., Adam N. M., Sahari B. B., et al. (2017). *New Design of a CNG-H-2-AIR Mixer for Internal Combustion Engines: An Experimental and Numerical Study*. Energies. 10(9), 1373.

17. Wang H., Yao M., Reitz R. D. (2013). *Development of a Reduced Primary Reference Fuel Mechanism for Internal Combustion Engine Combustion Simulations*. Energy Fuels. 27(12), 7843–7853.

18. Maghbouli A., Saray R. K., Shafee S., Ghafouri J. (2013). *Numerical Study of Combustion and Emission Characteristics of Dual-Fuel Engines Using 3D-CFD Models Coupled with Chemical Kinetics*. Fuel 106, 98–105.

19. Han Z. Y., Reitz R. D. (1997). *A Temperature Wall Function Formulation for Variable-Density Turbulent Flows with Application to Engine Convective Heat Transfer Modeling*. International Journal of Heat & Mass Transfer. 40(3), 613–625.

20. Han Z., Reitz R. D. (1995). Turbulence *Modeling of Internal Combustion Engines Using RNG K-E Models*. Combustion Science and Technology. 106, 267–95.

21. Butler T. D., Cloutman L. D., Dukowicz J. K., Ramshaw D.J. (1981). *Multidimensional numerical simulation of reactive flow in internal combustion engines*. Progress in Energy & Combustion ence. 7(4), 293–315.

22. Beale J. C., Reitz R. D. (1999). *Modeling Spray Atomization with the Kelvin-Helmholtz/Rayleigh-Taylor Hybrid Model*. Atomization and Sprays. 9(6), 623–650.

23. Feng S. (2017). *Numerical Study of the Performance and Emission of a Diesel-Syngas Dual Fuel Engin*e. Mathematical Problems in Engineering.10, 1–12.

24. Colket M. B., Spadaccini L. J. (2012). *Scramjet Fuels Autoignition Study*. Journal of Propulsion and Power. 17(2), 315–323.

25. Verhelst S., Joen C. T., Coillie J. V., et al. (2011). *A Correlation for the Laminar Burning Velocity for Use in Hydrogen Spark Ignition Engine Simulation*. International Journal of Hydrogen Energy. 36(1), 957–974.

26. D'Andrea T., Henshaw P. F., Ting S. K. (2004). *The Addition of Hydrogen to a Gasoline-Fuelled SI Engine*. International Journal of Hydrogen Energy. 29(14), 1541–1552.

27. Li W., Liu Z., Wang Z. (2016). *Experimental and Theoretical Analysis of the Combustion Process at Low Loads of a Diesel Natural Gas Dual-Fuel Engine*. Energy. 94, 728–741.

CONTACT WITH THE AUTHORS

Rui Zhao
e-mail: zhaorui@shmtu.edu.cn

Merchant Marine College,
Shanghai Maritime University,
1550 Haigang Ave, 201306 Shanghai
China

Leping Xu
e-mail: leping_xu@yeah.net

Merchant Marine College,
Shanghai Maritime University,
1550 Haigang Ave, 201306 Shanghai
China

Xiangwen Su
e-mail: xw.su@shcmd.com.cn

CSSC-MES Diesel Co. Ltd,
6 Xinyuan South Road, 201306 Shanghai
China

Shiquan Feng
e-mail: fengshiquan@outlook.com

School of Automotive Engineering,
Changshu Institute of Technology,
No. 99, 3rd South Ring Road, 215500 Suzhou
China

Changxiong Li
e-mail: fengshiquan@outlook.com

Merchant Marine College,
Shanghai Maritime University,
1550 Haigang Ave, 201306 Shanghai
China

Qinming Tan
e-mail: qmtan@shmtu.edu.cn

Merchant Marine College,
Shanghai Maritime University,
1550 Haigang Ave, 201306 Shanghai
China

Zhongcheng Wang
e-mail: wangzhongchengwzc@163.com

Merchant Marine College,
Shanghai Maritime University,
1550 Haigang Ave, 201306 Shanghai
China